BABAR-CONF-02/07
SLAC-PUB-9229
hep-ex/0205082
May, 2002

Measurements of Branching Fractions and *CP*-Violating Asymmetries in $B^0 \to \pi^+\pi^-$, $K^+\pi^-$, K^+K^- Decays

The *BABAR* Collaboration

May 23, 2002

Abstract

We present updated measurements of branching fractions and *CP*-violating asymmetries for neutral B meson decays to two-body final states of charged pions and kaons. The results are obtained from a data sample of about 60 million $\Upsilon(4S) \to B\overline{B}$ decays collected between 1999 and 2001 by the *BABAR* detector at the PEP-II asymmetric-energy B Factory at SLAC. The sample contains 124^{+16}_{-15} $\pi\pi$, 403 ± 24 $K\pi$, and $0.6^{+8.0}_{-7.4}$ KK candidates, from which we measure the following quantities:

$$\begin{aligned}
\mathcal{B}(B^0 \to \pi^+\pi^-) &= (5.4 \pm 0.7 \pm 0.4) \times 10^{-6}, \\
\mathcal{B}(B^0 \to K^+\pi^-) &= (17.8 \pm 1.1 \pm 0.8) \times 10^{-6}, \\
\mathcal{B}(B^0 \to K^+K^-) &< 1.1 \times 10^{-6}\ (90\%\,\text{C.L.}), \\
\mathcal{A}_{K\pi} &= -0.05 \pm 0.06 \pm 0.01\ [-0.14, +0.05]\,, \\
S_{\pi\pi} &= -0.01 \pm 0.37 \pm 0.07\ [-0.66, +0.62]\,, \\
C_{\pi\pi} &= -0.02 \pm 0.29 \pm 0.07\ [-0.54, +0.48]\,,
\end{aligned}$$

where the errors are statistical and systematic, respectively, and the asymmetry limits correspond to the 90% confidence level. These results are preliminary.

Presented at the 37^{th} Rencontres de Moriond on Electroweak Interactions and Unified Theories, 3/9—3/16/2002, Les Arcs, Savoie, France

Stanford Linear Accelerator Center, Stanford University, Stanford, CA 94309

Work supported in part by Department of Energy contract DE-AC03-76SF00515.

The *BABAR* Collaboration,

B. Aubert, D. Boutigny, J.-M. Gaillard, A. Hicheur, Y. Karyotakis, J. P. Lees, P. Robbe, V. Tisserand, A. Zghiche

Laboratoire de Physique des Particules, F-74941 Annecy-le-Vieux, France

A. Palano, A. Pompili

Università di Bari, Dipartimento di Fisica and INFN, I-70126 Bari, Italy

G. P. Chen, J. C. Chen, N. D. Qi, G. Rong, P. Wang, Y. S. Zhu

Institute of High Energy Physics, Beijing 100039, China

G. Eigen, I. Ofte, B. Stugu

University of Bergen, Inst. of Physics, N-5007 Bergen, Norway

G. S. Abrams, A. W. Borgland, A. B. Breon, D. N. Brown, J. Button-Shafer, R. N. Cahn, E. Charles, M. S. Gill, A. V. Gritsan, Y. Groysman, R. G. Jacobsen, R. W. Kadel, J. Kadyk, L. T. Kerth, Yu. G. Kolomensky, J. F. Kral, C. LeClerc, M. E. Levi, G. Lynch, L. M. Mir, P. J. Oddone, M. Pripstein, N. A. Roe, A. Romosan, M. T. Ronan, V. G. Shelkov, A. V. Telnov, W. A. Wenzel

Lawrence Berkeley National Laboratory and University of California, Berkeley, CA 94720, USA

T. J. Harrison, C. M. Hawkes, D. J. Knowles, S. W. O'Neale, R. C. Penny, A. T. Watson, N. K. Watson

University of Birmingham, Birmingham, B15 2TT, United Kingdom

T. Deppermann, K. Goetzen, H. Koch, B. Lewandowski, K. Peters, H. Schmuecker, M. Steinke

Ruhr Universität Bochum, Institut für Experimentalphysik 1, D-44780 Bochum, Germany

N. R. Barlow, W. Bhimji, N. Chevalier, P. J. Clark, W. N. Cottingham, B. Foster, C. Mackay, F. F. Wilson

University of Bristol, Bristol BS8 1TL, United Kingdom

K. Abe, C. Hearty, T. S. Mattison, J. A. McKenna, D. Thiessen

University of British Columbia, Vancouver, BC, Canada V6T 1Z1

S. Jolly, A. K. McKemey

Brunel University, Uxbridge, Middlesex UB8 3PH, United Kingdom

V. E. Blinov, A. D. Bukin, D. A. Bukin, A. R. Buzykaev, V. B. Golubev, V. N. Ivanchenko, A. A. Korol, E. A. Kravchenko, A. P. Onuchin, S. I. Serednyakov, Yu. I. Skovpen, A. N. Yushkov

Budker Institute of Nuclear Physics, Novosibirsk 630090, Russia

D. Best, M. Chao, D. Kirkby, A. J. Lankford, M. Mandelkern, S. McMahon, D. P. Stoker

University of California at Irvine, Irvine, CA 92697, USA

K. Arisaka, C. Buchanan, S. Chun

University of California at Los Angeles, Los Angeles, CA 90024, USA

D. B. MacFarlane, S. Prell, Sh. Rahatlou, G. Raven, V. Sharma

University of California at San Diego, La Jolla, CA 92093, USA

C. Campagnari, B. Dahmes, P. A. Hart, N. Kuznetsova, S. L. Levy, O. Long, A. Lu, M. A. Mazur, J. D. Richman, W. Verkerke

University of California at Santa Barbara, Santa Barbara, CA 93106, USA

J. Beringer, A. M. Eisner, M. Grothe, C. A. Heusch, W. S. Lockman, T. Pulliam, T. Schalk, R. E. Schmitz, B. A. Schumm, A. Seiden, M. Turri, W. Walkowiak, D. C. Williams, M. G. Wilson

University of California at Santa Cruz, Institute for Particle Physics, Santa Cruz, CA 95064, USA

E. Chen, G. P. Dubois-Felsmann, A. Dvoretskii, D. G. Hitlin, S. Metzler, J. Oyang, F. C. Porter, A. Ryd, A. Samuel, S. Yang, R. Y. Zhu

California Institute of Technology, Pasadena, CA 91125, USA

S. Jayatilleke, G. Mancinelli, B. T. Meadows, M. D. Sokoloff

University of Cincinnati, Cincinnati, OH 45221, USA

T. Barillari, P. Bloom, W. T. Ford, U. Nauenberg, A. Olivas, P. Rankin, J. Roy, J. G. Smith, W. C. van Hoek, L. Zhang

University of Colorado, Boulder, CO 80309, USA

J. Blouw, J. L. Harton, M. Krishnamurthy, A. Soffer, W. H. Toki, R. J. Wilson, J. Zhang

Colorado State University, Fort Collins, CO 80523, USA

T. Brandt, J. Brose, T. Colberg, M. Dickopp, R. S. Dubitzky, A. Hauke, E. Maly, R. Müller-Pfefferkorn, S. Otto, K. R. Schubert, R. Schwierz, B. Spaan, L. Wilden

Technische Universität Dresden, Institut für Kern- und Teilchenphysik, D-01062 Dresden, Germany

D. Bernard, G. R. Bonneaud, F. Brochard, J. Cohen-Tanugi, S. Ferrag, S. T'Jampens, Ch. Thiebaux, G. Vasileiadis, M. Verderi

Ecole Polytechnique, LLR, F-91128 Palaiseau, France

A. Anjomshoaa, R. Bernet, A. Khan, D. Lavin, F. Muheim, S. Playfer, J. E. Swain, J. Tinslay

University of Edinburgh, Edinburgh EH9 3JZ, United Kingdom

M. Falbo

Elon University, Elon College, NC 27244-2010, USA

C. Borean, C. Bozzi, L. Piemontese

Università di Ferrara, Dipartimento di Fisica and INFN, I-44100 Ferrara, Italy

E. Treadwell

Florida A&M University, Tallahassee, FL 32307, USA

F. Anulli,[1] R. Baldini-Ferroli, A. Calcaterra, R. de Sangro, D. Falciai, G. Finocchiaro, P. Patteri, I. M. Peruzzi,[2] M. Piccolo, Y. Xie, A. Zallo

Laboratori Nazionali di Frascati dell'INFN, I-00044 Frascati, Italy

S. Bagnasco, A. Buzzo, R. Contri, G. Crosetti, M. Lo Vetere, M. Macri, M. R. Monge, S. Passaggio, F. C. Pastore, C. Patrignani, E. Robutti, A. Santroni, S. Tosi

Università di Genova, Dipartimento di Fisica and INFN, I-16146 Genova, Italy

[1]Also with Università di Perugia, I-06100 Perugia, Italy

[2]Also with Università di Perugia, I-06100 Perugia, Italy

M. Morii

Harvard University, Cambridge, MA 02138, USA

R. Bartoldus, R. Hamilton, U. Mallik

University of Iowa, Iowa City, IA 52242, USA

J. Cochran, H. B. Crawley, J. Lamsa, W. T. Meyer, E. I. Rosenberg, J. Yi

Iowa State University, Ames, IA 50011-3160, USA

G. Grosdidier, A. Höcker, H. M. Lacker, S. Laplace, F. Le Diberder, V. Lepeltier, A. M. Lutz, S. Plaszczynski, M. H. Schune, S. Trincaz-Duvoid, G. Wormser

Laboratoire de l'Accélérateur Linéaire, F-91898 Orsay, France

R. M. Bionta, V. Brigljević , D. J. Lange, M. Mugge, K. van Bibber, D. M. Wright

Lawrence Livermore National Laboratory, Livermore, CA 94550, USA

A. J. Bevan, J. R. Fry, E. Gabathuler, R. Gamet, M. George, M. Kay, D. J. Payne, R. J. Sloane, C. Touramanis

University of Liverpool, Liverpool L69 3BX, United Kingdom

M. L. Aspinwall, D. A. Bowerman, P. D. Dauncey, U. Egede, I. Eschrich, G. W. Morton, J. A. Nash, P. Sanders, D. Smith

University of London, Imperial College, London, SW7 2BW, United Kingdom

J. J. Back, G. Bellodi, P. Dixon, P. F. Harrison, R. J. L. Potter, H. W. Shorthouse, P. Strother, P. B. Vidal

Queen Mary, University of London, E1 4NS, United Kingdom

G. Cowan, S. George, M. G. Green, A. Kurup, C. E. Marker, T. R. McMahon, S. Ricciardi, F. Salvatore, G. Vaitsas

University of London, Royal Holloway and Bedford New College, Egham, Surrey TW20 0EX, United Kingdom

D. Brown, C. L. Davis

University of Louisville, Louisville, KY 40292, USA

J. Allison, R. J. Barlow, J. T. Boyd, A. C. Forti, F. Jackson, G. D. Lafferty, N. Savvas, J. H. Weatherall, J. C. Williams

University of Manchester, Manchester M13 9PL, United Kingdom

A. Farbin, A. Jawahery, V. Lillard, J. Olsen, D. A. Roberts, J. R. Schieck

University of Maryland, College Park, MD 20742, USA

G. Blaylock, C. Dallapiccola, K. T. Flood, S. S. Hertzbach, R. Kofler, V. B. Koptchev, T. B. Moore, H. Staengle, S. Willocq

University of Massachusetts, Amherst, MA 01003, USA

B. Brau, R. Cowan, G. Sciolla, F. Taylor, R. K. Yamamoto

Massachusetts Institute of Technology, Laboratory for Nuclear Science, Cambridge, MA 02139, USA

M. Milek, P. M. Patel

McGill University, Montréal, QC, Canada H3A 2T8

F. Palombo, C. Vite

Università di Milano, Dipartimento di Fisica and INFN, I-20133 Milano, Italy

J. M. Bauer, L. Cremaldi, V. Eschenburg, R. Kroeger, J. Reidy, D. A. Sanders, D. J. Summers

University of Mississippi, University, MS 38677, USA

C. Hast, J. Y. Nief, P. Taras

Université de Montréal, Laboratoire René J. A. Lévesque, Montréal, QC, Canada H3C 3J7

H. Nicholson

Mount Holyoke College, South Hadley, MA 01075, USA

C. Cartaro, N. Cavallo,[3] G. De Nardo, F. Fabozzi, C. Gatto, L. Lista, P. Paolucci, D. Piccolo, C. Sciacca

Università di Napoli Federico II, Dipartimento di Scienze Fisiche and INFN, I-80126, Napoli, Italy

J. M. LoSecco

University of Notre Dame, Notre Dame, IN 46556, USA

J. R. G. Alsmiller, T. A. Gabriel

Oak Ridge National Laboratory, Oak Ridge, TN 37831, USA

J. Brau, R. Frey, E. Grauges , M. Iwasaki, C. T. Potter, N. B. Sinev, D. Strom

University of Oregon, Eugene, OR 97403, USA

F. Colecchia, F. Dal Corso, A. Dorigo, F. Galeazzi, M. Margoni, M. Morandin, M. Posocco, M. Rotondo, F. Simonetto, R. Stroili, E. Torassa, C. Voci

Università di Padova, Dipartimento di Fisica and INFN, I-35131 Padova, Italy

M. Benayoun, H. Briand, J. Chauveau, P. David, Ch. de la Vaissière, L. Del Buono, O. Hamon, Ph. Leruste, J. Ocariz, M. Pivk, L. Roos, J. Stark

Universités Paris VI et VII, Lab de Physique Nucléaire H. E., F-75252 Paris, France

P. F. Manfredi, V. Re, V. Speziali

Università di Pavia, Dipartimento di Elettronica and INFN, I-27100 Pavia, Italy

E. D. Frank, L. Gladney, Q. H. Guo, J. Panetta

University of Pennsylvania, Philadelphia, PA 19104, USA

C. Angelini, G. Batignani, S. Bettarini, M. Bondioli, F. Bucci, E. Campagna, M. Carpinelli, F. Forti, M. A. Giorgi, A. Lusiani, G. Marchiori, F. Martinez-Vidal, M. Morganti, N. Neri, E. Paoloni, M. Rama, G. Rizzo, F. Sandrelli, G. Simi, G. Triggiani, J. Walsh

Università di Pisa, Scuola Normale Superiore and INFN, I-56010 Pisa, Italy

M. Haire, D. Judd, K. Paick, L. Turnbull, D. E. Wagoner

Prairie View A&M University, Prairie View, TX 77446, USA

J. Albert, P. Elmer, C. Lu, V. Miftakov, S. F. Schaffner, A. J. S. Smith, A. Tumanov, E. W. Varnes

Princeton University, Princeton, NJ 08544, USA

[3]Also with Università della Basilicata, I-85100 Potenza, Italy

F. Bellini, G. Cavoto, D. del Re, R. Faccini,[4] F. Ferrarotto, F. Ferroni, M. A. Mazzoni, S. Morganti, G. Piredda, M. Serra, C. Voena

Università di Roma La Sapienza, Dipartimento di Fisica and INFN, I-00185 Roma, Italy

S. Christ, R. Waldi

Universität Rostock, D-18051 Rostock, Germany

T. Adye, N. De Groot, B. Franek, N. I. Geddes, G. P. Gopal, S. M. Xella

Rutherford Appleton Laboratory, Chilton, Didcot, Oxon, OX11 0QX, United Kingdom

R. Aleksan, S. Emery, A. Gaidot, S. F. Ganzhur, P.-F. Giraud, G. Hamel de Monchenault, W. Kozanecki, M. Langer, G. W. London, B. Mayer, B. Serfass, G. Vasseur, Ch. Yèche, M. Zito

DAPNIA, Commissariat à l'Energie Atomique/Saclay, F-91191 Gif-sur-Yvette, France

M. V. Purohit, A. W. Weidemann, F. X. Yumiceva

University of South Carolina, Columbia, SC 29208, USA

I. Adam, D. Aston, N. Berger, A. M. Boyarski, G. Calderini, M. R. Convery, D. P. Coupal, D. Dong, J. Dorfan, W. Dunwoodie, R. C. Field, T. Glanzman, S. J. Gowdy, T. Haas, T. Hadig, V. Halyo, T. Himel, T. Hryn'ova, M. E. Huffer, W. R. Innes, C. P. Jessop, M. H. Kelsey, P. Kim, M. L. Kocian, U. Langenegger, D. W. G. S. Leith, S. Luitz, V. Luth, H. L. Lynch, H. Marsiske, S. Menke, R. Messner, D. R. Muller, C. P. O'Grady, V. E. Ozcan, A. Perazzo, M. Perl, S. Petrak, H. Quinn, B. N. Ratcliff, S. H. Robertson, A. Roodman, A. A. Salnikov, T. Schietinger, R. H. Schindler, J. Schwiening, A. Snyder, A. Soha, S. M. Spanier, J. Stelzer, D. Su, M. K. Sullivan, H. A. Tanaka, J. Va'vra, S. R. Wagner, M. Weaver, A. J. R. Weinstein, W. J. Wisniewski, D. H. Wright, C. C. Young

Stanford Linear Accelerator Center, Stanford, CA 94309, USA

P. R. Burchat, C. H. Cheng, T. I. Meyer, C. Roat

Stanford University, Stanford, CA 94305-4060, USA

R. Henderson

TRIUMF, Vancouver, BC, Canada V6T 2A3

W. Bugg, H. Cohn

University of Tennessee, Knoxville, TN 37996, USA

J. M. Izen, I. Kitayama, X. C. Lou

University of Texas at Dallas, Richardson, TX 75083, USA

F. Bianchi, M. Bona, D. Gamba

Università di Torino, Dipartimento di Fisica Sperimentale and INFN, I-10125 Torino, Italy

L. Bosisio, G. Della Ricca, S. Dittongo, L. Lanceri, P. Poropat, L. Vitale, G. Vuagnin

Università di Trieste, Dipartimento di Fisica and INFN, I-34127 Trieste, Italy

R. S. Panvini

Vanderbilt University, Nashville, TN 37235, USA

[4]Also with University of California at San Diego, La Jolla, CA 92093, USA

C. M. Brown, P. D. Jackson, R. Kowalewski, J. M. Roney
University of Victoria, Victoria, BC, Canada V8W 3P6

H. R. Band, S. Dasu, M. Datta, A. M. Eichenbaum, H. Hu, J. R. Johnson, R. Liu, F. Di Lodovico, Y. Pan, R. Prepost, I. J. Scott, S. J. Sekula, J. H. von Wimmersperg-Toeller, S. L. Wu, Z. Yu
University of Wisconsin, Madison, WI 53706, USA

T. M. B. Kordich, H. Neal
Yale University, New Haven, CT 06511, USA

Recent measurements of the *CP*-violating asymmetry parameter sin2β by the *BABAR* [1] and Belle [2] collaborations established *CP* violation in the B^0 system. These measurements, as well as an updated result by *BABAR* [3] reported at this conference, are consistent with the Standard Model expectation based on measurements and theoretical estimates of the elements of the Cabibbo-Kobayashi-Maskawa [4] (CKM) quark-mixing matrix.

The study of B decays to charmless hadronic two-body final states will yield important information about the remaining angles (α and γ) of the Unitarity Triangle. In the Standard Model, the time-dependent *CP*-violating asymmetry in the decay $B^0 \to \pi^+\pi^-$ is related to the angle α, and ratios of branching fractions for various $\pi\pi$ and $K\pi$ decay modes are sensitive to the angle γ. In this paper, we update our previous measurements of branching fractions [5] and *CP*-violating asymmetries [6] in $B^0 \to \pi^+\pi^-$, $K^+\pi^-$, and K^+K^- decays[1] using a sample of 60 million $B\overline{B}$ pairs.

We reconstruct a sample of B mesons ($B_{\rm rec}$) decaying to the $h^+h'^-$ final state, where h and h' refer to π or K, and examine the remaining charged particles in each event to "tag" the flavor of the other B meson ($B_{\rm tag}$). The decay rate distribution $f_+\,(f_-)$ when $h^+h'^- = \pi^+\pi^-$ and $B_{\rm tag} = B^0\,(\overline{B}^0)$ is given by

$$f_\pm(\Delta t) = \frac{e^{-|\Delta t|/\tau}}{4\tau}[1 \pm S_{\pi\pi}\sin(\Delta m_d \Delta t) \mp C_{\pi\pi}\cos(\Delta m_d \Delta t)], \tag{1}$$

where τ is the mean B^0 lifetime, Δm_d is the eigenstate mass difference, and $\Delta t = t_{\rm rec} - t_{\rm tag}$ is the time between the $B_{\rm rec}$ and $B_{\rm tag}$ decays. The *CP*-violating parameters $S_{\pi\pi}$ and $C_{\pi\pi}$ are defined as

$$S_{\pi\pi} = \frac{2\,\mathcal{I}m\lambda}{1+|\lambda|^2} \quad \text{and} \quad C_{\pi\pi} = \frac{1-|\lambda|^2}{1+|\lambda|^2}. \tag{2}$$

If the decay proceeds purely through the $b \to uW^-$ tree process, then λ is given by

$$\lambda(B \to \pi^+\pi^-) = \left(\frac{V_{tb}^* V_{td}}{V_{tb} V_{td}^*}\right)\left(\frac{V_{ud}^* V_{ub}}{V_{ud} V_{ub}^*}\right). \tag{3}$$

In this case $C_{\pi\pi} = 0$ and $S_{\pi\pi} = \sin2\alpha$, where $\alpha \equiv \arg\,[-V_{\rm td}V_{\rm tb}^*/V_{\rm ud}V_{\rm ub}^*]$. In general, the $b \to dg$ penguin amplitude modifies both the magnitude and phase of λ, so that $C_{\pi\pi} \neq 0$ and $S_{\pi\pi} = \sqrt{1-C_{\pi\pi}^2}\sin 2\alpha_{\rm eff}$, where $\alpha_{\rm eff}$ depends on the magnitudes and relative strong and weak phases of the tree and penguin amplitudes. Several approaches have been proposed to obtain information on α in the presence of penguins [7].

The data sample used in this analysis consists of 55.6 fb^{-1}, corresponding to (60.2 $\pm$ 0.7) million $B\overline{B}$ pairs, collected on the $\Upsilon(4S)$ resonance with the *BABAR* detector at the SLAC PEP-II storage ring between October 1999 and December 2001. A detailed description of the detector is presented in Ref. [8]. Charged particle (track) momenta are measured in a tracking system consisting of a 5-layer double-sided silicon vertex tracker (SVT) and a 40-layer drift chamber (DCH) filled with a gas mixture of helium and isobutane. The SVT and DCH operate within a 1.5 T superconducting solenoidal magnet. Photons are detected in an electromagnetic calorimeter (EMC) consisting of 6580 CsI(Tl) crystals arranged in barrel and forward endcap subdetectors. The flux return for the solenoid is composed of multiple layers of iron and resistive plate chambers for the identification of muons and long-lived neutral hadrons. Tracks from the $B_{\rm rec}$ decay are identified as pions or kaons by the Cherenkov angle θ_c measured with a detector of internally reflected Cherenkov light (DIRC).

[1] Unless explicitly stated, charge conjugate decay modes are assumed throughout this paper.

Event selection is identical to that described in Ref. [6]. Candidate $B_{\rm rec}$ decays are reconstructed from pairs of oppositely-charged tracks forming a good quality vertex, where the $B_{\rm rec}$ four-vector is calculated assuming the pion mass for both tracks. We require each track to have an associated θ_c measurement with a minimum of six Cherenkov photons above background, where the average is approximately 30 for both pions and kaons. Protons are rejected based on θ_c and electrons are rejected based on dE/dx measurements in the tracking system, shower shape in the EMC, and the ratio of shower energy and track momentum. Background from the reaction $e^+e^- \to q\bar{q}$ ($q = u, d, s, c$) is suppressed by removing jet-like events from the sample: we define the center-of-mass (c.m.) angle θ_S between the sphericity axes of the B candidate and the remaining tracks and photons in the event, and require $|\cos\theta_S| < 0.8$, which removes 83% of the background. The total efficiency on signal events for all of the above selection is approximately 38%.

Signal decays are identified kinematically using two variables. We define a beam-energy substituted mass $m_{\rm ES} = \sqrt{E_{\rm b}^2 - \mathbf{p}_B^2}$, where the B candidate energy is defined as $E_{\rm b} = (s/2 + \mathbf{p}_i \cdot \mathbf{p}_B)/E_i$, $\sqrt{s}$ and E_i are the total energies of the e^+e^- system in the c.m. and laboratory frames, respectively, and $\mathbf{p}_i$ and $\mathbf{p}_B$ are the momentum vectors in the laboratory frame of the e^+e^- system and the $B_{\rm rec}$ candidate, respectively. Signal events are Gaussian distributed in $m_{\rm ES}$ with a mean near the B mass and a resolution of $2.6\,{\rm MeV}/c^2$, dominated by the beam energy spread. The background shape is parameterized by a threshold function [9] with a fixed endpoint given by the average beam energy.

We define a second kinematic variable ΔE as the difference between the energy of the $B_{\rm rec}$ candidate in the c.m. frame and $\sqrt{s}/2$. Signal $\pi\pi$ decays are Gaussian distributed with a mean value near zero. For decays with one (two) kaons, the distribution is shifted relative to $\pi\pi$ on average by $-45\,{\rm MeV}$ ($-91\,{\rm MeV}$), respectively, where the exact separation depends on the laboratory momentum of the kaon(s). The resolution on ΔE is approximately 26 MeV and is validated in large samples of fully reconstructed B decays. The background is parameterized by a quadratic function.

Candidate $h^+h'^-$ pairs selected in the region $5.2 < m_{\rm ES} < 5.3\,{\rm GeV}/c^2$ and $|\Delta E| < 0.15\,{\rm GeV}$ are used to extract yields and *CP*-violating asymmetries with an unbinned maximum likelihood fit. The total number of events in the fit region satisfying all of the above criteria is 17585.

To determine the flavor of the $B_{\rm tag}$ meson we use the same B-tagging algorithm used in the *BABAR* sin2β analysis [10]. The algorithm relies on the correlation between the flavor of the b quark and the charge of the remaining tracks in the event after removal of the $B_{\rm rec}$ candidate. We define five mutually exclusive tagging categories: `Lepton`, `Kaon`, `NT1`, `NT2`, and `Untagged`. `Lepton` tags rely on primary electrons and muons from semileptonic B decays, while `Kaon` tags exploit the correlation in the process $b \to c \to s$ between the net kaon charge and the charge of the b quark. The `NT1` (more certain tags) and `NT2` (less certain tags) categories are derived from a neural network that is sensitive to charge correlations between the parent B and unidentified leptons and kaons, soft pions, or the charge and momentum of the track with the highest c.m. momentum. The addition of `Untagged` events improves the signal yield estimates and provides a larger sample for determining background shape parameters directly in the maximum likelihood fit.

The quality of tagging is expressed in terms of the effective efficiency $Q = \sum_c \epsilon_c D_c^2$, where ϵ_c is the fraction of events tagged in category c and the dilution $D_c = 1 - 2w_c$ is related to the mistag fraction w_c. Table 1 summarizes the tagging performance in a data sample $B_{\rm flav}$ of fully reconstructed neutral B decays into $D^{(*)-}h^+$ ($h^+ = \pi^+, \rho^+, a_1^+$) and $J/\psi K^{*0}$ ($K^{*0} \to K^+\pi^-$) flavor eigenstates. We use the same tagging efficiencies and dilutions for signal $\pi\pi$, $K\pi$, and KK decays. Separate background efficiencies for each species are determined simultaneously with $S_{\pi\pi}$ and $C_{\pi\pi}$ in the maximum likelihood fit.

Table 1: Tagging efficiency ϵ, average dilution $D = 1/2\,(D_{B^0} + D_{\overline{B}^0})$, dilution difference $\Delta D = D_{B^0} - D_{\overline{B}^0}$, and effective tagging efficiency Q for signal events in each tagging category. The values are measured in the $B_{\rm flav}$ sample.

Category	$\epsilon\,(\%)$	$D\,(\%)$	$\Delta D\,(\%)$	$Q\,(\%)$
`Lepton`	11.1 ± 0.2	82.8 ± 1.8	-1.2 ± 3.0	7.6 ± 0.4
`Kaon`	34.7 ± 0.4	63.8 ± 1.4	1.8 ± 2.1	14.1 ± 0.6
`NT1`	7.6 ± 0.2	56.0 ± 3.0	-2.7 ± 4.7	2.4 ± 0.3
`NT2`	14.0 ± 0.3	25.4 ± 2.6	9.4 ± 3.8	0.9 ± 0.2
`Untagged`	32.6 ± 0.5	–	–	–
Total Q				25.0 ± 0.8

The time difference Δt is obtained from the measured distance between the z positions of the $B_{\rm rec}$ and $B_{\rm tag}$ decay vertices and the known boost of the e^+e^- system. The z position of the $B_{\rm tag}$ vertex is determined with an iterative procedure that removes tracks with a large contribution to the total χ^2. An additional constraint is constructed from the three-momentum and vertex position of the $B_{\rm rec}$ candidate, and the average e^+e^- interaction point and boost. For 99.5% of candidates with a reconstructed vertex the r.m.s. Δz resolution is $180\,\mu$m (1.1 ps). We require $|\Delta t| < 20$ ps and $\sigma_{\Delta t} < 2.5$ ps, where $\sigma_{\Delta t}$ is the error on Δt. The resolution function for signal candidates is a sum of three Gaussians, identical to the one described in Ref. [3], with parameters determined from a fit to the $B_{\rm flav}$ sample (including events in all five tagging categories). The background Δt distribution is parameterized as the sum of an exponential convolved with a Gaussian, and two additional Gaussians to account for tails. A common parameterization is used for all tagging categories, and the parameters are determined simultaneously with the *CP* parameters in the maximum likelihood fit. We find that 86% of background events are described by an effective lifetime of about 0.6 ps, while tails are described by 12 (2)% of events with a resolution of approximately 2 (8) ps.

Discrimination of signal from light-quark background is enhanced by the use of a Fisher discriminant $\mathcal{F}$ [5]. The discriminating variables are constructed from the scalar sum of the c.m. momenta of all tracks and photons (excluding tracks from the $B_{\rm rec}$ candidate) entering nine two-sided 10-degree concentric cones centered on the thrust axis of the $B_{\rm rec}$ candidate. The distribution of $\mathcal{F}$ for signal events is parameterized as a single Gaussian, with parameters determined from Monte Carlo simulated decays and validated with $B^- \to D^0\pi^-$ decays reconstructed in data. The background shape is parameterized as the sum of two Gaussians, with parameters determined directly in the maximum likelihood fit.

Identification of $h^+h'^-$ tracks as pions or kaons is accomplished with the Cherenkov angle measurement from the DIRC. We construct Gaussian probability density functions (PDFs) from the difference between measured and expected values of θ_c for the pion or kaon hypothesis, normalized by the resolution. The DIRC performance is parameterized using a sample of $D^{*+} \to D^0\pi^+$, $D^0 \to K^-\pi^+$ decays, reconstructed in data. The typical separation between pions and kaons varies from 8σ at 2 GeV/c to 2.5σ at 4 GeV/c, where σ is the average resolution on θ_c (Fig. 1).

We use an unbinned extended maximum likelihood fit to extract yields and *CP* parameters from the $B_{\rm rec}$ sample. The likelihood for candidate j tagged in category c is obtained by summing the product of event yield n_i, tagging efficiency $\epsilon_{i,c}$, and probability $\mathcal{P}_{i,c}$ over the eight possible signal

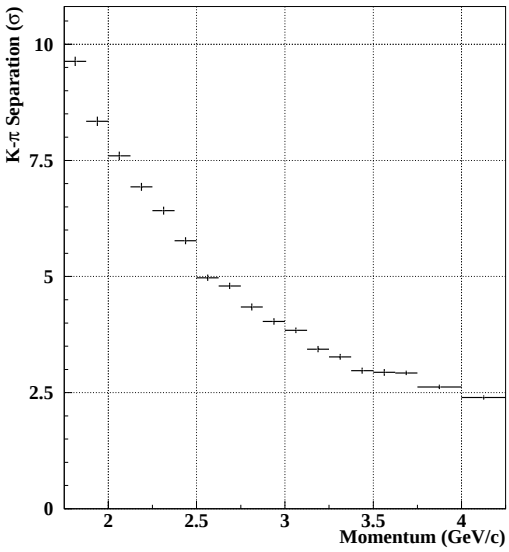

Figure 1: Variation of the separation between the kaon and pion Cherenkov angles with momentum, as obtained from a control sample of $D^{*+} \to D^0\pi^+$, $D^0 \to K^-\pi^+$ decays reconstructed in data.

and background hypotheses i (referring to $\pi\pi$, $K^+\pi^-$, $K^-\pi^+$, and KK decays),

$$\mathcal{L}_c = \exp\left(-\sum_i n_i\epsilon_{i,c}\right)\prod_j\left[\sum_i n_i\epsilon_{i,c}\mathcal{P}_{i,c}(\vec{x}_j;\vec{\alpha}_i)\right]. \tag{4}$$

For the $K^\mp\pi^\pm$ components, the yield is parameterized as $n_i = N_{K\pi}\left(1 \pm \mathcal{A}_{K\pi}\right)/2$, where $N_{K\pi} = N_{K^-\pi^+} + N_{K^+\pi^-}$ and $\mathcal{A}_{K\pi} \equiv (N_{K^-\pi^+} - N_{K^+\pi^-})/(N_{K^-\pi^+} + N_{K^+\pi^-})$. The probabilities $\mathcal{P}_{i,c}$ are evaluated as the product of PDFs for each of the independent variables $\vec{x}_j = \{m_{\rm ES}, \Delta E, \mathcal{F}, \theta_c^+, \theta_c^-, \Delta t\}$, where θ_c^+ and θ_c^- are the Cherenkov angles for the positively and negatively charged tracks. We use the same PDF parameters for θ_c^+ and θ_c^-. The total likelihood $\mathcal{L}$ is the product of likelihoods for each tagging category and the free parameters are determined by minimizing the quantity $-\ln\mathcal{L}$.

In order to minimize systematic error on the branching fraction measurements, we perform an initial fit without tagging or Δt information. A total of 16 parameters are varied in the fit, including signal and background yields (6 parameters) and asymmetries (2), and parameters for the background shapes in $m_{\rm ES}$ (1), ΔE (2), and $\mathcal{F}$ (5). Table 2 summarizes results for signal yields, total efficiencies, branching fractions, and $\mathcal{A}_{K\pi}$. The upper limit on the signal yield for $B^0 \to K^+K^-$ is given by the value of n^0 for which $\int_0^{n^0}\mathcal{L}_{\rm max}\,dn / \int_0^\infty \mathcal{L}_{\rm max}\,dn = 0.90$, where $\mathcal{L}_{\rm max}$ is the likelihood as a function of n, maximized with respect to the remaining fit parameters. The branching fraction upper limit is calculated by increasing the signal yield upper limit and reducing the efficiency by their respective systematic errors. The dominant systematic error on the branching fraction measurements is due to uncertainty in the shape of the θ_c PDF, while the dominant error on $\mathcal{A}_{K\pi}$ is due to possible charge bias in track and θ_c reconstruction. All measurements reported

Table 2: Summary of results for total detection efficiencies (Eff), fitted signal yields N_S, measured branching fractions $\mathcal{B}$, and the $K\pi$ charge asymmetry $\mathcal{A}_{K\pi}$. The sample corresponds to (60.2 ± 0.7) million $B\overline{B}$ pairs produced, where equal branching fractions for $\Upsilon(4S) \to B^0\overline{B}^0$ and B^+B^- are assumed. The statistical and systematic errors on $\mathcal{A}_{K\pi}$ are added in quadrature when calculating the 90% confidence level (C.L.).

Mode	Eff (%)	N_S	$\mathcal{B}(10^{-6})$	$\mathcal{A}_{K\pi}$	$\mathcal{A}_{K\pi}$ 90% C.L.
$\pi^+\pi^-$	38.5 ± 0.7	$124^{+16\,+7}_{-15\,-9}$	$5.4 \pm 0.7 \pm 0.4$		
$K^+\pi^-$	37.6 ± 0.7	$403 \pm 24 \pm 15$	$17.8 \pm 1.1 \pm 0.8$	$-0.05 \pm 0.06 \pm 0.01$	$[-0.14, +0.05]$
K^+K^-	36.7 ± 0.7	$0.6^{+8.0}_{-7.4}$ (< 15.6)	< 1.1 (90% C.L.)		

in Table 2 are consistent with our previous results reported in Ref. [5].

Figure 2 shows distributions of $m_{\rm ES}$ and ΔE after a cut on likelihood ratios. We define $\mathcal{R}_{\rm sig} = \sum_s n_s\mathcal{P}_s / \sum_i n_i\mathcal{P}_i$ and $\mathcal{R}_k = n_k\mathcal{P}_k / \sum_s n_s\mathcal{P}_s$, where $\sum_s$ ($\sum_i$) indicates a sum over signal (all) hypotheses, and $\mathcal{P}_k$ indicates the probability for signal hypothesis k. The probabilities include the PDFs for θ_c, $\mathcal{F}$, and $m_{\rm ES}$ (ΔE) when plotting ΔE ($m_{\rm ES}$). The selection is defined by optimizing the signal significance with respect to $\mathcal{R}_{\rm sig}$ and $\mathcal{R}_k$. The solid curve in each plot represents the fit projection after correcting for the efficiency of the additional selection (approximately 67% for $\pi\pi$ and 88% for $K\pi$).

The time-dependent CP asymmetries $S_{\pi\pi}$ and $C_{\pi\pi}$ are determined from a second fit including tagging and Δt information, with the yields and $\mathcal{A}_{K\pi}$ fixed to the results of the first fit. The Δt PDF for signal $\pi^+\pi^-$ decays is given by Eq. 1, modified to include the dilution and dilution difference for each tagging category, and convolved with the signal resolution function. The Δt PDF for signal $K\pi$ events takes into account B^0–$\overline{B}^0$ mixing, depending on the charge of the kaon and the flavor of $B_{\rm tag}$. We parameterize the Δt distribution in $B^0 \to K^+K^-$ decays as an exponential convolved with the resolution function.

A total of 34 parameters are varied in the fit, including the values of $S_{\pi\pi}$ and $C_{\pi\pi}$, separate background tagging efficiencies for $\pi\pi$, $K\pi$, and KK events (12), parameters for the background Δt resolution function (8), and parameters for the background shapes in $m_{\rm ES}$ (5), ΔE (2), and $\mathcal{F}$ (5). The signal tagging efficiencies and dilutions are fixed to the values in Table 1, while τ and Δm_d are fixed to their PDG values [11]. To validate the analysis technique, we measure τ and Δm_d in the $B_{\rm rec}$ sample and find $\tau = (1.66 \pm 0.09)$ ps and $\Delta m_d = (0.517 \pm 0.062)\hbar\,{\rm ps}^{-1}$. Figure 3 shows the asymmetry $\mathcal{A}_{\rm mix} = (N_{\rm unmixed} - N_{\rm mixed})/(N_{\rm unmixed} + N_{\rm mixed})$ in a sample of events enhanced in $B \to K\pi$ decays. The curve shows the expected oscillation given the value of Δm_d measured in the full sample.

The fit yields

$$\begin{aligned} S_{\pi\pi} &= -0.01 \pm 0.37\,({\rm stat}) \pm 0.07\,({\rm syst})\ [-0.66, +0.62]\,, \\ C_{\pi\pi} &= -0.02 \pm 0.29\,({\rm stat}) \pm 0.07\,({\rm syst})\ [-0.54, +0.48]\,. \end{aligned}$$

For each parameter, we also calculate the 90% confidence level (C.L.) interval taking into account the systematic error. The correlation between $S_{\pi\pi}$ and $C_{\pi\pi}$ is -13%. Systematic uncertainties on $S_{\pi\pi}$ and $C_{\pi\pi}$ are dominated by uncertainty in the shape of the θ_c PDF. Since we measure asymmetries near zero, multiplicative systematic errors have also been evaluated (0.05). We sum in quadrature multiplicative errors, evaluated at one standard deviation, with the additive systematic

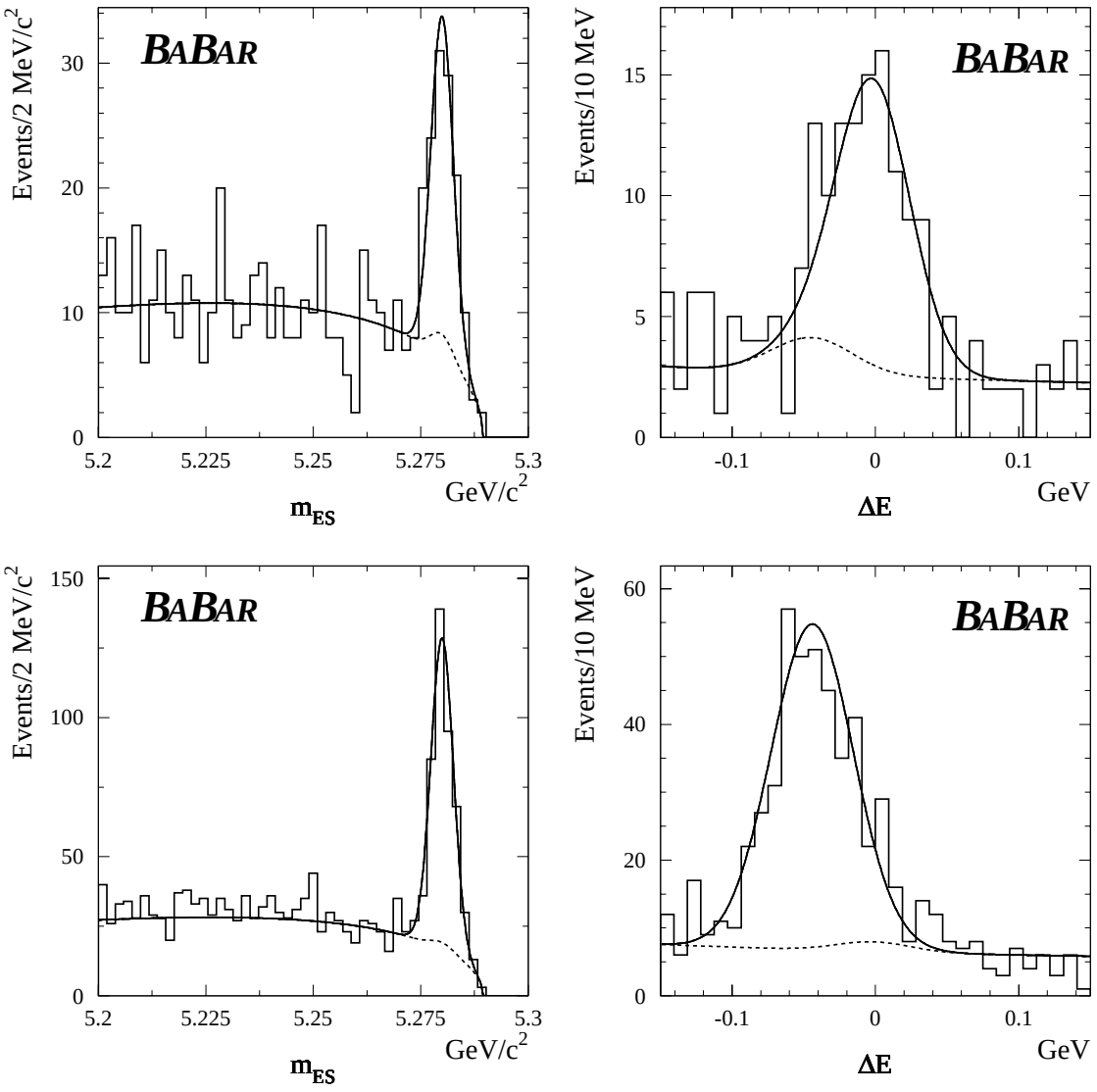

Figure 2: Distributions of $m_{\rm ES}$ and ΔE (histograms) for events enhanced in signal $\pi\pi$ (top) and $K\pi$ (bottom) decays based on the likelihood ratio selection described in the text. Solid curves represent projections of the maximum likelihood fit result after accounting for the efficiency of the additional selection, while dashed curves represent $q\bar{q}$ and $\pi\pi \leftrightarrow K\pi$ cross-feed background.

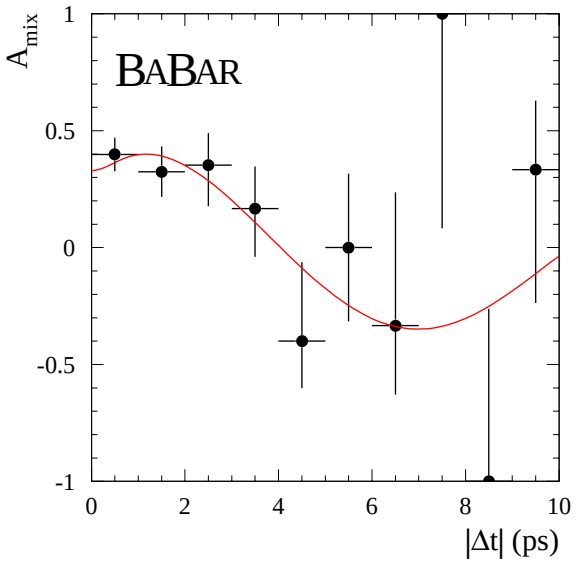

Figure 3: The asymmetry $\mathcal{A}_{\rm mix}$ between mixed and unmixed events in a sample enhanced in $K\pi$ decays. The curve indicates the expected oscillation corresponding to $\Delta m_d = 0.517\,\hbar\,{\rm ps}^{-1}$. The dilution from $q\bar{q}$ events is evident in the reduced amplitude near $|\Delta t| = 0$.

uncertainties. Figure 4 shows the Δt distributions and the asymmetry $\mathcal{A}_{\pi\pi}(\Delta t) = (N_{B^0}(\Delta t) - N_{\overline{B}^0}(\Delta t))/(N_{B^0}(\Delta t) + N_{\overline{B}^0}(\Delta t))$ for tagged events enhanced in signal $\pi\pi$ decays. The selection procedure is the same as Fig. 2, with the likelihoods defined including the PDFs for θ_c, $\mathcal{F}$, $m_{\rm ES}$, and ΔE.

In summary, we have presented updated measurements of branching fractions and *CP*-violating asymmetries in $B^0 \to \pi^+\pi^-$, $K^+\pi^-$, and K^+K^- decays. All results are consistent with previous measurements. Our measurement of $\mathcal{A}_{K\pi}$ is currently the most accurate available, and disfavors theoretical models that predict a large asymmetry [12, 13].

We are grateful for the excellent luminosity and machine conditions provided by our PEP-II colleagues, and for the substantial dedicated effort from the computing organizations that support *BABAR*. The collaborating institutions wish to thank SLAC for its support and kind hospitality. This work is supported by DOE and NSF (USA), NSERC (Canada), IHEP (China), CEA and CNRS-IN2P3 (France), BMBF (Germany), INFN (Italy), NFR (Norway), MIST (Russia), and PPARC (United Kingdom). Individuals have received support from the A. P. Sloan Foundation, Research Corporation, and Alexander von Humboldt Foundation.

References

[1] *BABAR* Collaboration, B. Aubert *et al.*, Phys. Rev. Lett. **87**, 091801 (2001).

[2] BELLE Collaboration, K. Abe *et al.*, Phys. Rev. Lett. **87**, 091802 (2001).

[3] *BABAR* Collaboration, B. Aubert *et al.*, hep-ex/0203007 (2002).

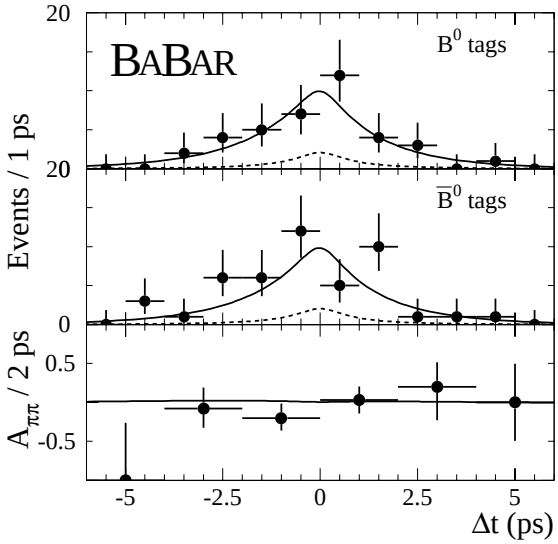

Figure 4: Distributions of Δt for events enhanced in signal $\pi\pi$ decays based on the likelihood ratio selection described in the text. The top two plots show events (points with errors) with $B_{\rm tag} = B^0$ or $\overline{B}^0$. Solid curves represent projections of the maximum likelihood fit, dashed curves represent the sum of $q\bar{q}$ and $K\pi$ background events. The bottom plot shows $\mathcal{A}_{\pi\pi}(\Delta t)$ for data (points with errors) and the fit projection.

[4] N. Cabibbo, Phys. Rev. Lett. **10**, 531 (1963); M. Kobayashi and T. Maskawa, Prog. Th. Phys. **49**, 652 (1973).

[5] *BABAR* Collaboration, B. Aubert *et al.*, Phys. Rev. Lett. **87**, 151802 (2001).

[6] *BABAR* Collaboration, B. Aubert *et al.*, Phys. Rev. D **65**, 051502 (2002).

[7] M. Gronau and D. London, Phys. Rev. Lett. **65**, 3381 (1990); Y. Grossman and H.R. Quinn, Phys. Rev. D **58**, 017504 (1998); J. Charles, Phys. Rev. D **59**, 054007 (1999); M. Gronau, D. London, N. Sinha, and R. Sinha, Phys. Lett. B **514**, 315 (2001); M. Beneke, G. Buchalla, M. Neubert, and C.T. Sachrajda, Nucl. Phys. B **606**, 245 (2001).

[8] *BABAR* Collaboration, B. Aubert *et al.*, Nucl. Instr. and Methods A **479**, 1 (2002).

[9] ARGUS Collaboration, H. Albrecht *et al.*, Z. Phys. C **48**, 543 (1990).

[10] *BABAR* Collaboration, B. Aubert *et al.*, hep-ex/0201020, to appear in Phys. Rev. D **.**

[11] Particle Data Group, D.E. Groom *et al.*, Eur. Phys. Jour. C **15**, 1 (2000).

[12] Y.Y. Keum, H-n. Li, and A.I. Sanda, Phys. Rev. D **63**, 054008 (2001).

[13] M. Ciuchini *et al.*, Phys. Lett. B **515**, 33 (2001).